CHAPTER 9

CERAMIC MATERIALS

Ceramic Structures

Because ceramics are composed of at least two elements, and often more, their crystal structures are generally more complex than those for metals.

The atomic bonding in these materials ranges from purely ionic to totally covalent; many ceramics exhibit a combination of these two bonding types, the degree of ionic character being dependent on the electronegativities of the atoms.

Table 12.1 presents the percent ionic character for several common ceramic materials; these values were determined using Equation 2.10 and the electronegativities in Figure 2.7.

Table 12.1 For Several Ceramic Materials, Percent Ionic Character of the Interatomic Bonds

Material	*Percent Ionic Character*
CaF_2	89
MgO	73
NaCl	67
Al_2O_3	63
SiO_2	51
Si_3N_4	30
ZnS	18
SiC	12

$$\%\ \text{ionic character} = \{1 - \exp[-(0.25)(X_A - X_B)^2]\} \times 100 \qquad (2.10)$$

IA								VIII			IB	IIB	IIIA	IVA	VA	VIA	VIIA	0
1 H 2.1	IIA																	2 He –
3 Li 1.0	4 Be 1.5												5 B 2.0	6 C 2.5	7 N 3.0	8 O 3.5	9 F 4.0	10 Ne –
11 Na 0.9	12 Mg 1.2	IIIB	IVB	VB	VIB	VIIB					IB	IIB	13 Al 1.5	14 Si 1.8	15 P 2.1	16 S 2.5	17 Cl 3.0	18 Ar –
19 K 0.8	20 Ca 1.0	21 Sc 1.3	22 Ti 1.5	23 V 1.6	24 Cr 1.6	25 Mn 1.5	26 Fe 1.8	27 Co 1.8	28 Ni 1.8	29 Cu 1.9	30 Zn 1.6	31 Ga 1.6	32 Ge 1.8	33 As 2.0	34 Se 2.4	35 Br 2.8	36 Kr –	
37 Rb 0.8	38 Sr 1.0	39 Y 1.2	40 Zr 1.4	41 Nb 1.6	42 Mo 1.8	43 Tc 1.9	44 Ru 2.2	45 Rh 2.2	46 Pd 2.2	47 Ag 1.9	48 Cd 1.7	49 In 1.7	50 Sn 1.8	51 Sb 1.9	52 Te 2.1	53 I 2.5	54 Xe –	
55 Cs 0.7	56 Ba 0.9	57–71 La–Lu 1.1–1.2	72 Hf 1.3	73 Ta 1.5	74 W 1.7	75 Re 1.9	76 Os 2.2	77 Ir 2.2	78 Pt 2.2	79 Au 2.4	80 Hg 1.9	81 Tl 1.8	82 Pb 1.8	83 Bi 1.9	84 Po 2.0	85 At 2.2	86 Rn –	
87 Fr 0.7	88 Ra 0.9	89–102 Ac–No 1.1–1.7																

Figure 2.7 The electronegativity values for the elements. (Adapted from Linus Pauling, *The Nature of the Chemical Bond*, 3rd edition. Copyright 1939 and 1940, 3rd edition copyright © 1960, by Cornell University. Used by permission of the publisher, Cornell University Press.)

Applications of Ceramics

Most ceramic materials fall into an application–classification scheme that includes the following groups: glasses, structural clay products, whitewares, refractories, abrasives, cements, and the newly developed advanced ceramics. Figure 13.1

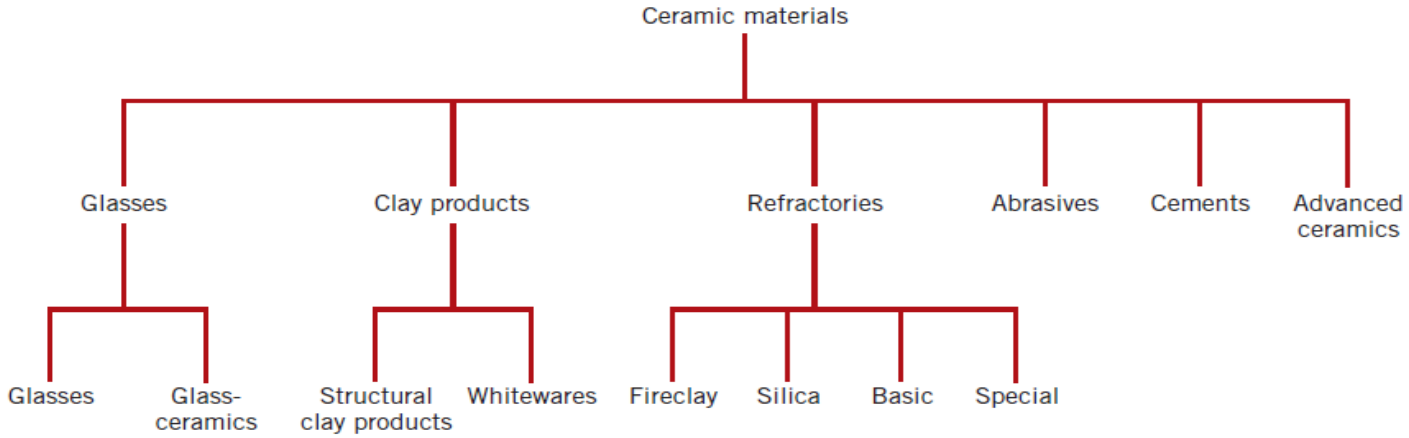

Figure 13.1 Classification of ceramic materials on the basis of application.

There are many different ways to classify ceramics. One way is to define ceramics based on their class of chemical compounds (e.g., oxides, carbides, nitrides, sulfides, fluorides, etc.). Another way, which we will use here, is to classify ceramics by their major function (Table 15-1).

TABLE 15–1 *Functional classification of ceramics**

Function	Application	Examples of Ceramics
Electrical	Capacitor dielectrics	$BaTiO_3$, $SrTiO_3$, Ta_2O_5
	Microwave dielectrics	$Ba(Mg_{1/3}Ta_{2/3})O_3$, $Ba(Zn_{1/3}Ta_{2/3})O_3$
		$BaTi_4O_9$, $Ba_2Ti_9O_{20}$, $Zr_xSn_{1-x}TiO_4$, Al_2O_3
	Conductive oxides	In-doped SnO_2 (*ITO*)
	Superconductors	$YBa_2Cu_3O_{7-x}$ (*YBCO*)
	Electronic packaging	Al_2O_3
	Insulators	Porcelain
	Solid-oxide fuel cells	ZrO_2, $LaCrO_3$
	Piezoelectric	$Pb(Zr_xTi_{1-x})O_3$ (*PZT*), $Pb(Mg_{1/3}Nb_{2/3})O_3$
	Electro-optical	*PLZT*, $LiNbO_3$
Magnetic	Recording media	γ-Fe_2O_3, CrO_2 ("chrome" cassettes)
	Ferrofluids, credit cards	Fe_3O_4
	Circulators, isolators	Nickel zinc ferrite
	Inductors, magnets	Manganese zinc ferrite
Optical	Fiber optics	Doped SiO_2
	Glasses	SiO_2 based
	Lasers	Al_2O_3, yttrium aluminum garnate (*YAG*)
	Lighting	Al_2O_3, glasses
Automotive	Oxygen sensors, fuel cells	ZrO_2
	Catalyst support	Cordierite
	Spark plugs	Al_2O_3
	Tires	SiO_2
	Windshields/windows	SiO_2 based glasses
Mechanical/Structural	Cutting tools	WC-Co cermets
		Silicon-aluminum-oxynitride (*Sialon*)
		Al_2O_3
	Composites	SiC, Al_2O_3, silica glass fibers
	Abrasives	SiC, Al_2O_3, diamond, BN, $ZrSiO_4$
Biomedical	Implants	Hydroxyapatite
	Dentistry	Porcelain, Al_2O_3
	Ultrasound imaging	*PZT*
Construction	Buildings	Concrete
		Glass
		Sanitaryware
Others	Defense applications	*PZT*, B_4C
	Armor materials	
	Sensors	SnO_2
	Nuclear	UO_2
		Glasses for waste disposal
	Metals processing	Alumina and silica-based refractories, oxygen sensors, casting molds, etc.
Chemical	Catalysis	Various oxides (Al_2O_3, ZrO_2, ZnO, TiO_2)
	Air, liquid filtration	
	Sensors	
	Paints, rubber	
Domestic	Tiles, sanitaryware, whiteware, kitchenware, pottery, art, jewelry	Clay, alumina, and silica-based ceramics, glass-ceramics, diamond, ruby, cubic zirconia, and other crystals

*Acronyms are indicated in italics.

Ceramics are used in a wide range of technologies such as refractories, spark plugs, dielectrics in capacitors, sensors, abrasives, and magnetic recording media.

Ceramics are also used as coatings. **Glazes** are ceramic coatings applied to glass objects; **enamels** are ceramic coatings applied to metallic objects.

Alumina and silica are the most widely used ceramic materials and, , there are numerous applications listed in Table 15-1 that depend upon the use of these two ceramics.

CRYSTAL STRUCTURES

For those ceramic materials for which the atomic bonding is predominantly ionic, the crystal structures composed of electrically charged ions instead of atoms.

The metallic ions, or **cations,** are positively charged, because they have given up their valence electrons to the nonmetallic ions, or **anions,** which are negatively charged.

Two characteristics of the component ions in crystalline ceramic materials influence the crystal structure:
1-The magnitude of the electrical charge on each of the component ions.
2- The relative sizes of the cations and anions.

Stable ceramic crystal structures form when those anions surrounding a cation are all in contact with that cation, as illustrated in Figure 12.1.

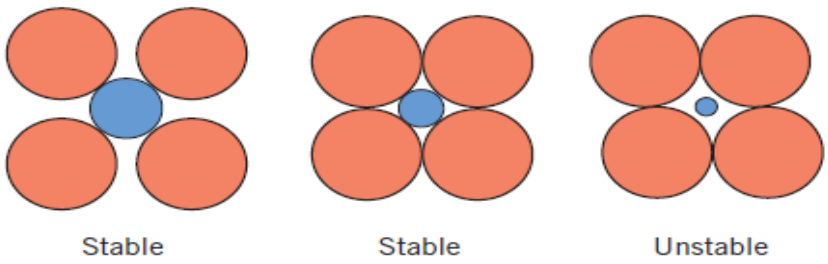

Figure 12.1 Stable and unstable anion–cation coordination configurations. Red circles represent anions; blue circles denote cations.

CERAMIC PHASE DIAGRAMS

Phase diagrams have been experimentally determined for a large number of ceramic systems. For binary or two-component phase diagrams, it is frequently the case that the two components are compounds that share a common element, often oxygen. These diagrams may have configurations similar to metal–metal systems, and they are interpreted in the same way Figure 12.24.

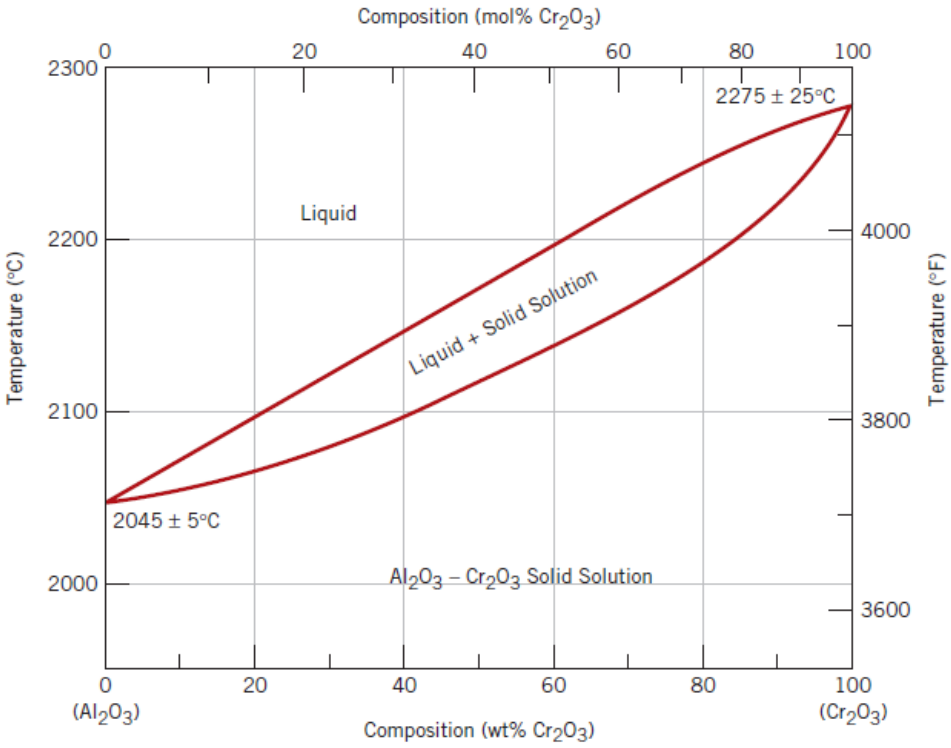

Figure 12.24 The aluminum oxide–chromium oxide phase diagram. (Adapted from E. N. Bunting, "Phase Equilibria in the System Cr_2O_3–Al_2O_3," *Bur. Standards J. Research*, **6**, 1931, p. 948.)

IMPERFECTIONS IN CERAMICS

Atomic Point Defects

Because ceramic materials contain ions of at least two kinds, defects for each ion type may occur.

Anion and cation vacancies and a cation interstitial are represented in Figure 12.20.

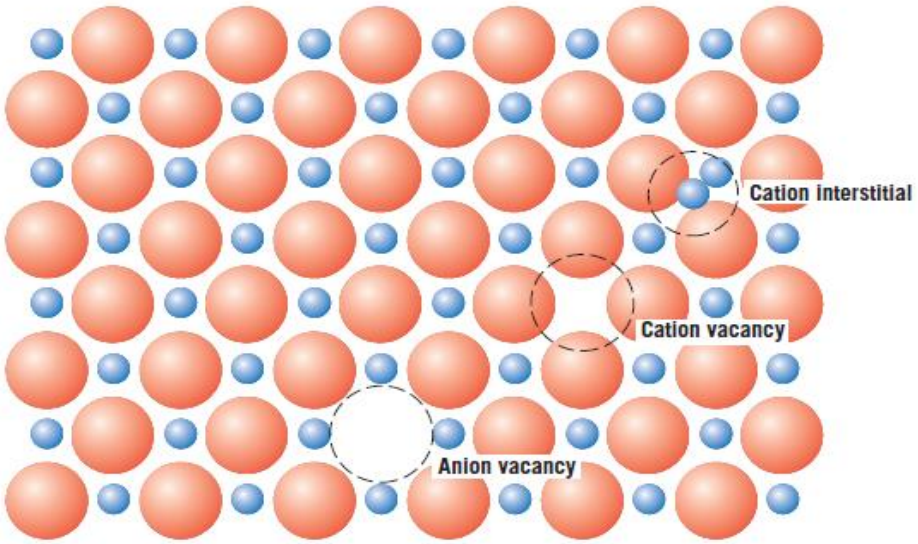

Figure 12.20 Schematic representations of cation and anion vacancies and a cation interstitial. (From W. G. Moffatt, G. W. Pearsall, and J. Wulff, *The Structure and Properties of Materials*, Vol. I, *Structure*, p. 78. Copyright © 1964 by John Wiley & Sons, New York. Reprinted by permission of John Wiley & Sons, Inc.)

The expression **defect structure** is often used to designate the types and concentrations of atomic defects in ceramics.

Electroneutrality is the state that exists when there are equal numbers of positive and negative charges from the ions.

Defects in ceramics do not occur alone:

a- One such type of defect involves a cation–vacancy and a cation–interstitial pair. This is called a **Frenkel defect** (Figure 12.21), being formed by a cation leaving its normal position and moving into an interstitial site. There is no change in charge because the cation maintains the same positive charge as an interstitial.

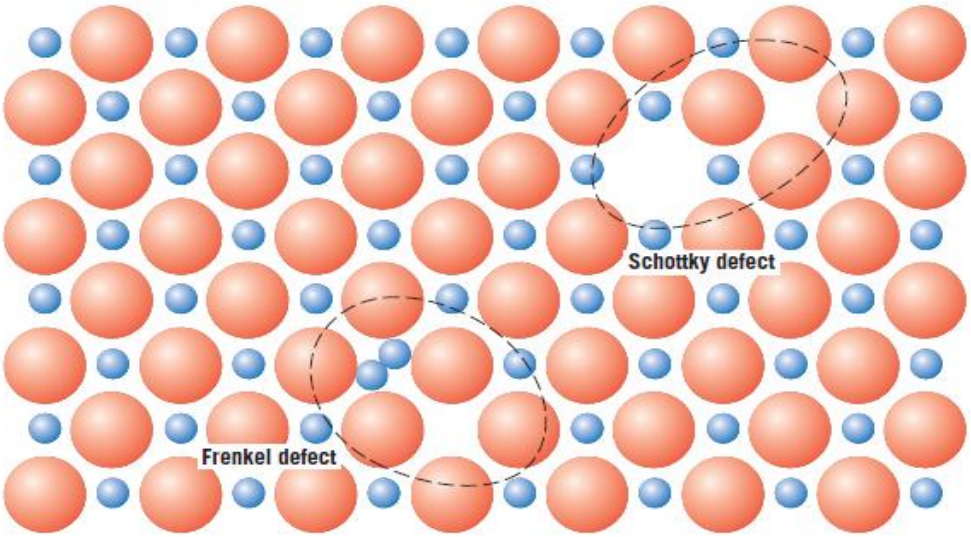

Figure 12.21 Schematic diagram showing Frenkel and Schottky defects in ionic solids. (From W. G. Moffatt, G. W. Pearsall, and J. Wulff, *The Structure and Properties of Materials*, Vol. I, *Structure*, p. 78. Copyright © 1964 by John Wiley & Sons, New York. Reprinted by permission of John Wiley & Sons, Inc.)

b- A cation vacancy–anion vacancy pair known as a **Schottky defect,** Figure 12.21, created by removing one cation and one anion from the interior of the crystal and then placing them both at an external surface.

Mechanical Properties

BRITTLE FRACTURE OF CERAMICS

At room temperature, both crystalline and noncrystalline ceramics almost always fracture before any plastic deformation can occur in response to an applied tensile load.

The brittle fracture process consists of the formation and propagation of cracks through the cross section of material in a direction perpendicular to the applied load.

The measure of a ceramic material's ability to resist fracture when a crack is present is specified in terms of fracture toughness. The plane strain fracture toughness K_{Ic},

$$K_{Ic} = Y\sigma\sqrt{\pi a} \qquad (12.5)$$

where Y is a dimensionless parameter or function that depends on both specimen and crack geometries, σ is the applied stress, and a is the length of a surface crack or half of the length of an internal crack. Crack propagation will not occur as long as the right-hand side of Equation 12.5 is less than the plane strain fracture toughness of the material. Plane strain fracture toughness values for ceramic materials are smaller than for metals; typically they are below 10 MPa$\sqrt{\text{m}}$ (9 ksi$\sqrt{\text{in.}}$). Val-

STRESS–STRAIN BEHAVIOR

Flexural Strength

The stress–strain behavior of brittle ceramics is not usually ascertained by a tensile test for three reasons.

1- It is difficult to prepare and test specimens having the required geometry.

2- It is difficult to grip brittle materials without fracturing them.

3- Ceramics fail after only about 0.1% strain.

The stress at fracture using this flexure test is known as the **flexural strength, *modulus of rupture, fracture strength,* or *bend strength,*** an important mechanical parameter for brittle ceramics.

Transverse bending test is most frequently employed, in which a rod specimen having either a circular or rectangular cross section is bent until fracture using a three- or four-point loading technique Figure 12.32.

For a **rectangular cross section**, the flexural strength σ_{fs} is equal to

$$\sigma_{fs} = \frac{3F_f L}{2bd^2} \qquad (12.7a)$$

Where F_f is the load at fracture, L is the distance between support points, and the other parameters are as indicated in Figure 12.32.

For a circular **cross section**, then

$$\sigma_{fs} = \frac{F_f L}{\pi R^3} \qquad (12.7b)$$

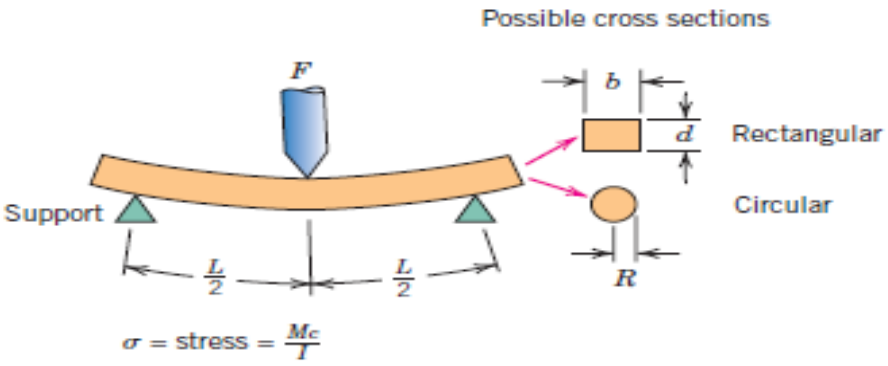

σ = stress = $\frac{Mc}{I}$

where M = maximum bending moment
c = distance from center of specimen to outer fibers
I = moment of inertia of cross section
F = applied load

	M	c	I	σ
Rectangular	$\frac{FL}{4}$	$\frac{d}{2}$	$\frac{bd^3}{12}$	$\frac{3FL}{2bd^2}$
Circular	$\frac{FL}{4}$	R	$\frac{\pi R^4}{4}$	$\frac{FL}{\pi R^3}$

Figure 12.32 A three-point loading scheme for measuring the stress–strain behavior and flexural strength of brittle ceramics, including expressions for computing stress for rectangular and circular cross sections.

Characteristic flexural strength values for several ceramic materials are given in Table 12.5.

Table 12.5 Tabulation of Flexural Strength (Modulus of Rupture) and Modulus of Elasticity for Ten Common Ceramic Materials

	Flexural Strength		*Modulus of Elasticity*	
Material	***MPa***	***ksi***	***GPa***	***10^6 psi***
Silicon nitride (Si_3N_4)	250–1000	35–145	304	44
Zirconia[a] (ZrO_2)	800–1500	115–215	205	30
Silicon carbide (SiC)	100–820	15–120	345	50
Aluminum oxide (Al_2O_3)	275–700	40–100	393	57
Glass-ceramic (Pyroceram)	247	36	120	17
Mullite ($3Al_2O_3$–$2SiO_2$)	185	27	145	21
Spinel ($MgAl_2O_4$)	110–245	16–35.5	260	38
Magnesium oxide (MgO)	105[b]	15[b]	225	33
Fused silica (SiO_2)	110	16	73	11
Soda-lime glass	69	10	69	10

[a] Partially stabilized with 3 mol% Y_2O_3.

[b] Sintered and containing approximately 5% porosity.

Elastic Behavior

The elastic stress–strain behavior for ceramic materials using these flexure tests is similar to the tensile test results for metals:

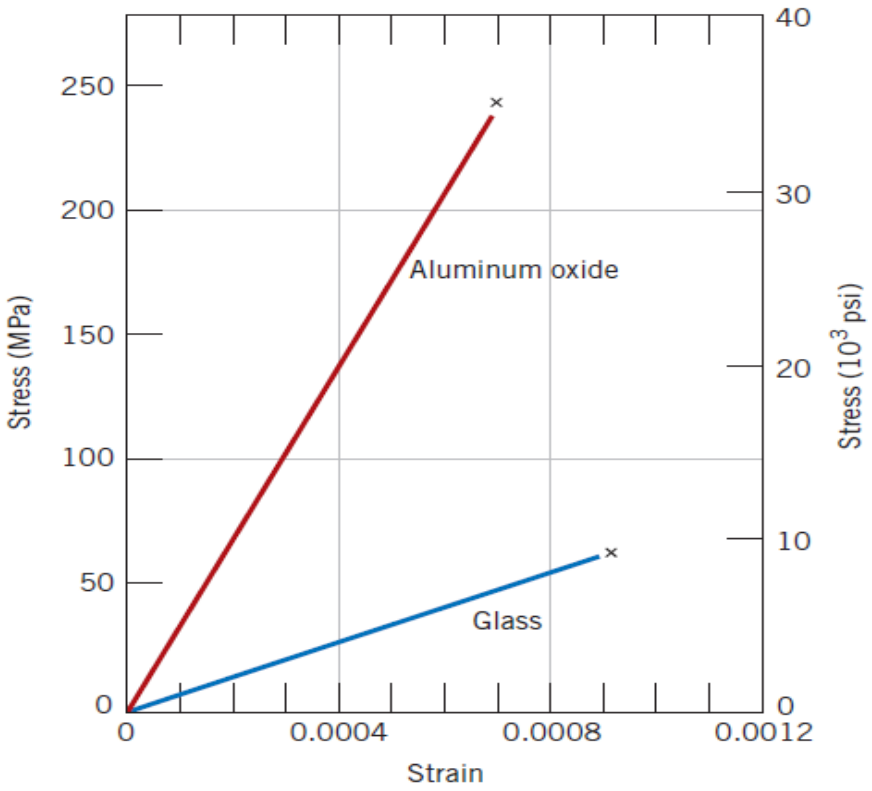

Figure 12.33 Typical stress–strain behavior to fracture for aluminum oxide and glass.

A linear relationship exists between stress and strain. Figure 12.33 compares the stress–strain behavior to fracture for aluminum oxide and glass.

The slope in the elastic region is the modulus of elasticity; the range of moduli of elasticity for ceramic materials is between about 70 and 500 GPa (10×10^6 and 70×10^6 psi), being slightly higher than for metals.

Table 12.5 lists values for several ceramic materials.

From **Figure 12.33** note that neither material experiences plastic deformation prior to fracture.

MISCELLANEOUS MECHANICAL CONSIDERATIONS

Influence of Porosity

Any residual porosity will have a deleterious influence on both the elastic properties and strength.

For example, for some ceramic materials the magnitude of the modulus of elasticity E decreases with volume fraction porosity P according to

$$E = E_0(1 - 1.9P + 0.9P^2) \qquad (12.9)$$

where E_0 is the modulus of elasticity of the nonporous material.

Hardness

Accurate hardness measurements are difficult to conduct inasmuch as ceramic materials are brittle and highly susceptible to cracking when indenters are forced into their surfaces

Hardnesses of this class of materials are measured using **Vickers** and **Knoop** techniques that employ indenters having pyramidal shapes.

The most desirable mechanical characteristic of ceramics is their hardness; the hardest known materials belong to this group.

These materials are often utilized when an abrasive or grinding action is required.

Creep

Often ceramic materials experience creep deformation as a result of exposure to stresses (usually compressive) at elevated temperatures.

The time– deformation creep behavior of ceramics is similar to that of metals.

Creep occurs at higher temperatures in ceramics.

QUESTIONS and ANSWERS

Q1-

A three-point bending test is performed on a glass specimen having a rectangular cross section of height d = 5 mm and width b = 10 mm; the distance between support points is 45 mm.
(a) Compute the flexural strength if the load at fracture is 290 N.
(b) The point of maximum deflection Δy occurs at the center of the specimen and is described by

$$\Delta y = \frac{FL^3}{48EI}$$

where E is the modulus of elasticity and I is the cross-sectional moment of inertia. Compute **Δy** at a load of 266 N.

Solution

(a) For this portion of the problem we are asked to compute the flexural strength for a glass specimen that is subjected to a three-point bending test. The flexural strength (Equation 12.7a) is just

$$\sigma_{fs} = \frac{3F_f L}{2bd^2}$$

for a rectangular cross-section. Using the values given in the problem statement,

$$\sigma_{fs} = \frac{(3)(290\ \text{N})(45 \times 10^{-3}\ \text{m})}{(2)(10 \times 10^{-3}\ \text{m})(5 \times 10^{-3}\ \text{m})^2} = 7.83 \times 10^7\ \text{N/m}^2 = 78.3\ \text{MPa}\quad (10{,}660\ \text{psi})$$

(b) We are now asked to compute the maximum deflection. From Table 12.5, the elastic modulus (E) for glass is 69 GPa (10×10^6 psi). Also, the moment of inertia for a rectangular cross section (Figure 12.32) is just

$$I = \frac{bd^3}{12}$$

Thus,

$$\Delta y = \frac{FL^3}{48E\left(\frac{bd^3}{12}\right)} = \frac{FL^3}{4Ebd^3}$$

$$= \frac{(266\ \text{N})(45 \times 10^{-3}\ \text{m})^3}{(4)(69 \times 10^9\ \text{N/m}^2)(10 \times 10^{-3}\ \text{m})(5 \times 10^{-3}\ \text{m})^3}$$

$$= 7.0 \times 10^{-5}\ \text{m} = 7.0 \times 10^{-2}\ \text{mm}\ (2.5 \times 10^{-3}\ \text{in.})$$

Q2-

A circular specimen of MgO is loaded using a three-point bending mode. Compute the minimum possible radius of the specimen without fracture, given that the applied load is 425 N (95.5 lb_f), the flexural strength is 105 MPa (15,000 psi), and the separation between load points is 50 mm (2.0 in.).

Solution

We are asked to calculate the maximum radius of a circular specimen of MgO that is loaded using three-point bending. Solving for R from Equation 12.7b

$$R = \left[\frac{F_f L}{\sigma_{fs} \pi}\right]^{1/3}$$

which, when substituting the parameters stipulated in the problem statement, yields

$$R = \left[\frac{(425\ \text{N})(50 \times 10^{-3}\ \text{m})}{(105 \times 10^6\ \text{N/m}^2)(\pi)}\right]^{1/3}$$

$$= 4.0 \times 10^{-3}\ \text{m} = 4.0\ \text{mm}\ (0.16\ \text{in.})$$

Q3-

A three-point bending test was performed on an aluminum oxide specimen having a circular cross section of radius 3.5 mm (0.14 in.); the specimen fractured at a load of 950 N (215 lb_f) when the distance between the support points was 50 mm (2.0 in.). Another test is to be performed on a specimen of this same material, but one that has a square cross section of 12 mm (0.47 in.) length on each edge. At what load would you expect this specimen to fracture if the support point separation is 40 mm (1.6 in.)?

Solution

For this problem, the load is given at which a circular specimen of aluminum oxide fractures when subjected to a three-point bending test; we are then are asked to determine the load at which a specimen of the same material having a square cross-section fractures. It is first necessary to compute the flexural strength of the aluminum oxide, Equation 12.7b, and then, using this value, we may calculate the value of F_f in Equation 12.7a.

From Equation 12.7b

$$\sigma_{fs} = \frac{F_f L}{\pi R^3}$$

$$= \frac{(950\ \text{N})(50 \times 10^{-3}\ \text{m})}{(\pi)(3.5 \times 10^{-3}\ \text{m})^3} = 352 \times 10^6\ \text{N/m}^2 = 352\ \text{MPa}\quad (50{,}000\ \text{psi})$$

Now, solving for F_f from Equation 12.7a, realizing that $b = d = 12$ mm, yields

$$F_f = \frac{2\sigma_{fs} d^3}{3L}$$

$$= \frac{(2)(352 \times 10^6\ \text{N/m}^2)(12 \times 10^{-3}\ \text{m})^3}{(3)(40 \times 10^{-3}\ \text{m})} = 10{,}100\ \text{N}\quad (2165\ \text{lb}_f)$$

Q4-

(a) A three-point transverse bending test is conducted on a cylindrical specimen of aluminum oxide having a reported flexural strength of 390 MPa (56,600 psi). If the specimen radius is 2.5 mm (0.10 in.) and the support point separation distance is 30 mm (1.2 in.), predict whether or not you would expect the specimen to fracture when a load of 620 N (140 lb_f) is applied. Justify your prediction.

(b) Would you be 100% certain of the prediction in part (a)? Why or why not?

Solution

(a) This portion of the problem asks that we determine whether or not a cylindrical specimen of aluminum oxide having a flexural strength of 390 MPa (56,600 psi) and a radius of 2.5 mm will fracture when subjected to a load of 620 N in a three-point bending test; the support point separation is given as 30 mm. Using Equation 12.7b we will calculate the value of σ; if this value is greater than σ_{fs} (390 MPa), then fracture is expected to occur. Employment of Equation 12.7b yields

$$\sigma = \frac{FL}{\pi R^3}$$

$$= \frac{(620\ \text{N})(30 \times 10^{-3}\ \text{m})}{(\pi)(2.5 \times 10^{-3}\ \text{m})^3} = 379 \times 10^6\ \text{N/m}^2 = 379\ \text{MPa}\quad (53{,}500\ \text{psi})$$

Since this value is less than the given value of σ_{fs} (390 MPa), then fracture is not predicted.

(b) The certainty of this prediction is not 100% because there is always some variability in the flexural strength for ceramic materials, and since this value of σ (379 MPa) is relatively close to σ_{fs} (390 MPa) then there is some chance that fracture will occur.